Biomedical Microdevices 6:1, 67–74, 2004

Microscale Transport and Sorting by Kinesin Molecular Motors

*Lili Jia,[1] Samira G. Moorjani,[2] Thomas N. Jackson,[1,3] and William O. Hancock[2]**

[1]Departments of Electrical Engineering, [2]Bioengineering, and [3]Materials Research Institute, The Pennsylvania State University, University Park, PA 16802

E-mail: wohbio@engr.psu.edu

Abstract. **As biomolecular detection systems shrink in size, there is an increasing demand for systems that transport and position materials at micron- and nanoscale dimensions. Our goal is to combine cellular transport machinery—kinesin molecular motors and microtubules—with integrated optoelectronics into a hybrid biological/engineered microdevice that will bind, transport, and detect specific proteins, DNA/RNA molecules, viruses, or cells. For microscale transport, 1.5 μm deep channels were created with SU-8 photoresist on glass, kinesin motors adsorbed to the bottom of the channels, and the channel walls used to bend and redirect microtubules moving over the immobilized motors. Novel channel geometries were investigated as a means to redirect and sort microtubules moving in these channels. We show that DC and AC electric fields are sufficient to transport microtubules in solution, establishing an approach for redirecting microtubules moving in channels. Finally, we inverted the geometry to demonstrate that kinesins can transport gold nanowires along surface immobilized microtubules, providing a model for nanoscale directed assembly.**

Key Words. **microfabrication, microtubule, electrophoresis, dielectrophoresis, microelectronics**

Introduction

As the amount of genomic sequence data and the understanding of specific DNA sequences grow, there is an increasing need for systems that can detect and purify minute quantities of genetic material. Current methods that have the greatest sensitivity include PCR-based approaches, which achieve maximal sensitivity (Marras et al., 1999), and DNA microarrays, which can analyze the levels of many targets in parallel (Schena et al., 1995). Because of the increasing use of these tests in detecting biohazards, biowarfare agents, and food pathogens, as well as in clinical diagnostics, there is a major thrust in building miniature, inexpensive, and even disposable devices for detection and purification of specific DNA or RNA targets, proteins or isolated cells. These ''lab-on-a-chip'' systems require miniaturizing processes such as sample delivery, material transport, biomolecular separation, and analyte detection, and integrating them into a single microdevice.

To enable such an integrated detection and purification system, we are employing kinesin biomolecular motors and microtubules. In cells, kinesins transport cargo such as vesicles, protein complexes and chromosomes along microtubules, using the energy of ATP hydrolysis. These motors move at roughly ~ 0.5 μm/sec (Howard et al., 1989), generate single motor forces of 6–8 pN (Svoboda et al., 1993; Meyhöfer and Howard, 1995) and in principle are capable of generating cumulative forces on the order of nN per μm^2 (Hancock and Howard, 1998; Limberis and Stewart, 2000). Kinesins' tracks, microtubules are 25 nm diameter cylindrical polymers of the protein tubulin that can be many microns long and can be polymerized *in vitro* from purified tubulin. A recurring theme in bio-nanotechnology and bio-MEMS is the need to manipulate matter at micron and nanoscale dimensions. Because nature has already solved this problem, we hope to take cellular machinery—kinesins and microtubules—and reconstitute this transport in microfabricated devices.

For designing microscale devices, molecular motor-based transport potentially offers distinct advantages over traditional microfluidics. Microfluidics requires external power to drive pumps and utilizes the inertia of the fluid itself to generate and control fluid flows, thus transporting particles within the flow. However, at these low Reynolds number regimes, inertial effects are minimal and viscous effects dominate, requiring high pumping pressures, especially for smaller channels. Additionally, such bulk flow transports all solutes together and requires creative flow profiles to generate separations. In contrast, molecular motors directly use their fuel (ATP hydrolysis) only at the site of action, and if the motors are not interacting with their tracks, they hydrolyze negligible amounts of fuel (Hackney, 1988). Furthermore, microtubule-based motility, which occurs in the absence of bulk flow, is specific—only microtubules and those molecules bound to them are transported, leaving the bulk solution behind. These transport characteristics suggest that biological motors may offer a new paradigm for transport in hybrid biological/engineered devices and that they may be used

*Corresponding author.

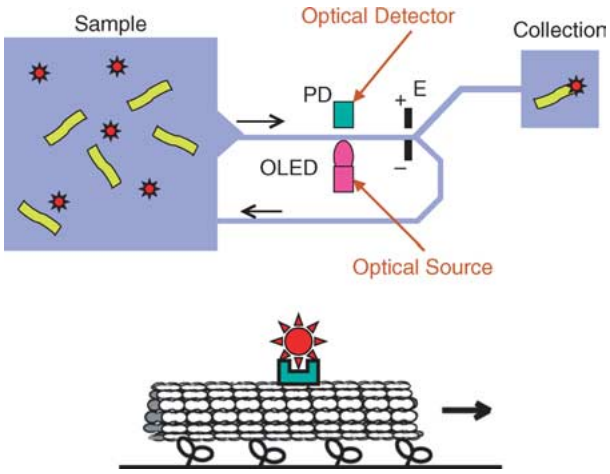

Fig. 1. *Diagram of motor-based detection and purification scheme. Top shows integrated system including sample chamber containing microtubules and analyte, motor-functionalized channels, organic LED exciter and photodiode (PD) detector, and electrodes (E) to direct cargo-laden microtubules to the collection chamber. Bottom shows the kinesin-based transport that will drive the system.*

to organize and assemble nanoscale synthetic particles and materials. The microdevice design presented here builds upon work by ourselves and others to interface molecular motors with engineered surfaces and to optimize microtubule transport along microfabricated features (Dennis et al., 1999; Limberis and Stewart, 2000; Stracke et al., 2000; Hess et al., 2001; Hiratsuka et al., 2001; Brown and Hancock, 2002; Clemmens et al., 2003; Moorjani et al., 2003).

Figure 1 shows a diagram of a hybrid biological/engineered system designed to isolate, transport and sort particular DNA/RNA molecules, proteins, viruses or cells from a heterogeneous sample. A small volume of cell lysate or tissue is inserted into the sample chamber, together with microtubules that are functionalized to bind the analyte of interest. Microtubules are transported by kinesin motors through microfabricated channels, the cargo is detected by embedded organic LEDs and photodiodes, sorted using electric fields at bifurcations in the channels, and then delivered to a collection chamber for analysis, sequencing, culturing, or other processing. Building such a system involves designing fluorescently labeled biomolecules with the necessary optical properties, optimizing the surface chemistry to both passivate and enable functional motor activity on surfaces, microfabricating prototypes of these devices, and adapting the microelectronics processing and fabrication to build the excitation and detection circuitry in these channels.

This paper presents the ground work towards constructing such a device. Microlithography is used to pattern channels on glass, kinesin motors are deposited in the channels, and novel channel architectures are employed to orient, redirect and sort microtubules traveling in these channels. To enable sorting of cargo-loaded from empty microtubules, we explore the forces imposed on microtubules by DC and AC electric fields. Finally, in addition to transporting microtubules in channels, we also demonstrate that the system can be inverted and used to transport kinesin-functionalized gold nanowires along immobilized microtubules. The tools developed here provide building blocks for realizing more complex bio/engineered hybrid devices for biomolecule transport and nanoscale assembly applications.

Materials and Methods

Motility assays

Full-length, His-tagged *Drosophila melanogaster* kinesin heavy chain was expressed in bacteria and purified as previously described (Hancock and Howard, 1998). Tubulin was purified from bovine brain, fluorescently labeled with rhodamine, and polymerized and taxol stabilized as previously described (Williams and Lee, 1982; Hyman et al., 1991; Howard et al., 1993). BRB80 buffer (80 mM PIPES, 1 mM EDTA, 1 mM $MgCl_2$, pH 6.9) was used for most solutions, a lower ionic strength BRB12 (12 mM K-PIPES, 1 mM EGTA and 2 mM $MgCl_2$, pH 6.9) was used for a portion of the electrophoresis and dielectrophoresis experiments. For microtubule motility, motors were adsorbed to surfaces at a concentration of 3.7 μg/ml (total protein from Coomassie stained gels) or 1 nM active concentration (as determined by radionucleotide binding, Coy et al., 1999), in the presence of 0.2 mg/ml casein, 0.1 mM ATP, 0.1% Triton X-100, and 150 mM potassium acetate. After a 5-minute incubation, taxol-stabilized microtubules (32 nM tubulin concentration, length 5–20 μm) were infused in the presence of 1 mM ATP, 0.2 mg/ml casein, 10 μM taxol, and antifade cocktail (20 mM D-glucose, 0.02 mg/ml glucose oxidase, 0.008 mg/ml catalase, 0.5% β-mercaptoethanol).

Microtubule observation

Microtubule movement within the channels was visualized by two optical techniques—differential interference contrast (DIC) and fluorescence microscopy using a Nikon E600 microscope (1.3 NA, 100X objective) coupled to a Hamamatsu 2400–87 intensified CCD camera and an Argus-20 video processing unit. Images were saved on VHS videotape and analyzed off-line. The simultaneous use of DIC to visualize the channel walls and fluorescence to image the microtubules allowed analysis of microtubule-wall interactions directly from the video.

Results and Discussion

Microtubule transport in microfabricated channels

The first geometry for extracting useful work from kinesins and microtubules is the microtubule gliding assay, in which motors are immobilized and microtubules are propelled across the surface (Allen et al., 1981; Vale et al., 1985; Howard et al., 1989). To obtain useful work from this system, it is necessary to guide microtubules in appropriate directions and to proper destinations. There has been work from a number of labs towards this goal, including depositing PTFE on glass (Dennis et al., 1999), fabricating steps and edges in silicon (Stracke et al., 2000), patterning motors on functionalized surfaces (Clemmens et al., 2003), and patterning channels in photoresist (Hiratsuka et al., 2001) and epoxy (Hess et al., 2001). We have also recently reported the use of the epoxy-based photoresist SU-8 to pattern 1.5 μm deep microchannels on glass substrates (Moorjani et al., 2003). The channels are then functionalized with kinesin motor proteins, which transport microtubules along them. The patterned SU-8 limits motility to the glass surfaces (channel bottoms) and the steep channel walls ($\sim 90°$) prevents microtubules from climbing out of the channels.

Based on this previous work, we have designed microchannels with a variety of geometric patterns to direct the movement of microtubules, including patterns designed to give unidirectional motion. Figure 2 shows SEM images of the vertical sidewall of a microfabricated channel patterned in SU-8 photoresist on glass, and structures designed to rectify the direction of microtubule movement. In these directional rectifiers, microtubules entering from the left will be guided along the wall, while those entering from the right will collide with the wall and be turned around.

Figure 3 shows the successful redirection of a moving microtubule by an arrowhead structure visualized by video fluorescence microscopy. A microtubule can be seen moving upward inside the arrowhead, bumping into the photoresist wall, and being redirected back into the channel. This result, which is consistent with the work of Hiratsuka et al. (2001) who demonstrated directional rectification by arrowheads fabricated in SAL601 e-beam photoresist, shows that SU-8 can also be used to construct intricate patterns to redirect microtubule motion. Shorter length microtubules were also observed rotating inside the channels in some cases, indicating that a narrower channel design may maximize unidirectional transport. A capped channel design may also be useful to prevent microtubules from diffusing away after colliding with the channel walls.

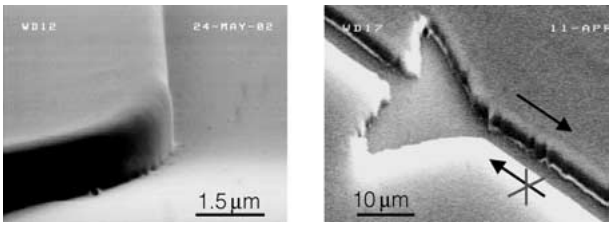

Fig. 2. *SEM showing patterned SU-8 photoresist on glass. Image at left shows the vertical sidewall of a microfabricated channel. Image at right shows structures designed to rectify the direction of microtubule movement.*

Fig. 3. *Rectifying microtubule movements by arrowhead structures. A microtubule can be seen moving upward inside the arrowhead, bumping into the photoresist wall, and being redirected back into the channel. Rhodamine-labeled microtubules and SU-8 channel walls were imaged using simultaneous fluorescence and differential interference contrast microscopy.*

Sorting microtubules with DC electric fields

The eventual goal of this microtubule transport work is to attach cargo to the microtubules and transport the cargo to desired locations. Hence, the next level of control over microtubule motion is to sort cargo-laden microtubules from unloaded microtubules. This sorting will be useful for concentrating analytes or selecting rare species from complex lysates. Here we examine redirecting and sorting microtubules by electrophoresis and dielectrophoresis.

Microtubules have a net negative charge at physio-

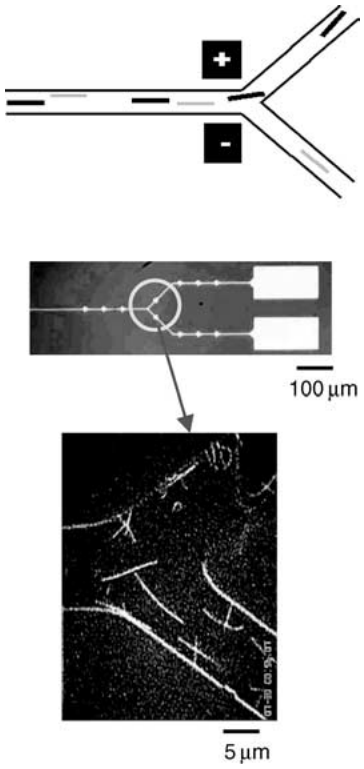

Fig. 4. Top: Y-junction designed to direct cargo-loaded microtubules by an electric field. Middle: Y-junction image taken under optical microscope. Bottom: microtubules observed moving inside Y-junction under fluorescence microscope.

logical pH, predicted to be 48 e^- per tubulin dimer based on the bovine tubulin amino acid sequence (Lowe, 2001). This translates to 84,000 e^- per micron length of microtubule. The strategy for sorting cargo-laden from empty microtubules will be to create bifurcations in the microfabricated channels and steer microtubules to either arm using an electric field oriented perpendicular to the direction of movement (Figure 4). Previously, Stracke et al. (2002) demonstrated that microtubules suspended in buffer in DC electric fields move toward the positive electrode and that under some conditions microtubules moving over a surface of immobilized kinesins can also be redirected by a static electric field. To demonstrate the feasibility of microtubule movements in bifurcated channels, we have fabricated Y-junction channels and observed the random motion of microtubules over kinesin coated glass surface in the channel, as shown in Figure 4. The next step is to determine whether electric field forces are sufficient to redirect a microtubule moving in such a bifurcation.

The key mechanical feature here is that as microtubules move over motor-coated surfaces, the front end is free from the surface and, under Brownian motion, searches over the surface for new motors to bind. The flexural rigidity of microtubules and the high motor densities normally employed ($\sim$ 100 motors/μm^2) in these assays results in fairly straight trajectories under normal conditions. However, by lowering the motor surface density to maximize the length of the microtubule's free front end, it should be possible to use electric fields to bend the filaments and direct microtubules at these bifurcations.

To show the feasibility of this approach, we can calculate the magnitude of the electric field needed to steer such a microtubule. Modeling the end of the microtubule as a cantilever that has one end clamped by the motors bound to it and the other end free, the force imposed by an electric field is analogous to the force of gravity on a horizontal cantilever, which can be calculated to be (Fitzgerald, 1982):

$$y_{\max} = \frac{FL^4}{8EI}, \tag{1}$$

where $y_{\max}$ is the maximum deflection, F is the force per unit length of the beam (equal to qE_{perp}, where E_{perp} is the electric field perpendicular to the microtubule) and EI is the flexural rigidity of microtubules, which has been measured to be 3.0×10^{-23} N-m^2 (Gittes, 1993). A 1 μm segment of microtubule consists of 1,750 tubulin dimers (Nogales et al., 1999), so a microtubule has a charge per unit length, q, of 1.35×10^{-8} C/m.

If a long microtubule moving over a sparse layer of motors has a 1 μm long free end, it can be calculated that the field strength sufficient to deflect the free end a distance of 0.1 μm is 1.8×10^3 V/m, an easily attainable field. One significant uncertainty in this calculation is the reduction in the charge due to shielding by cations, though this can be reduced somewhat by lowering the ionic strength of the solution. Other variables to optimize are the microtubule length, the surface density of motors, and the distance between the electrode pair and the bifurcation.

To test microtubule transport in a DC electric field, we used photolithography to fabricate gold microelectrodes with different geometries on glass microscope slides. First, a 5 $\sim$ 10 nm Cr adhesion layer was deposited by ion mill (Oxford) sputtering followed by 100 nm Au. After the fabrication of electrodes, electrical connections were made through conductive tape from the glass slide to a printed circuit (PC) board, and a power supply connected to this board (Figure 5). The electrodes were designed to have long bus-bars with the same geometry as the connecting tape and the PC board was also designed with identical electrode spacing. The conducting tape was bonded to the electrodes and the PC board using a heating bonder, and a flow cell was constructed on the glass slide using a microscope coverslip and two-sided tape for spacers. Rhodamine-

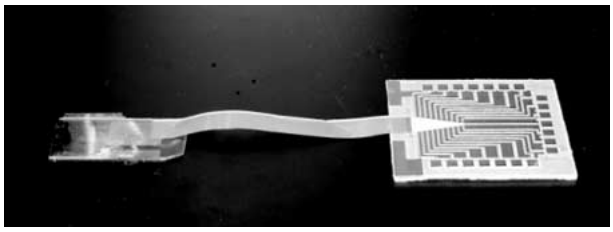

Fig. 5. *Microfabricated slide with flex connect and signal connector, the size of the glass slide used is 50 × 25 cm.*

labeled microtubules were suspended in BRB12 buffer and injected into the flow cell. The sample was then transferred to the fluorescence microscope and DC and AC electric fields were applied to the electrodes through cable connections and PC board.

In a DC electric field of 6×10^4 V/m (3V potential with 50 μm electrode spacing) microtubules of length ~ 10 μm moved toward the positive electrode at speeds of roughly 5 μm/s and accumulated there (Figure 6). To determine how the electrophoretic forces achieved in this experiment compare to our predictions, we can compare the electrophoretic force F_{EP} to the drag force F_{Drag}. For a microtubule moving at a constant speed, v, in an electric field $E, F_{EP} = F_{\text{Drag}}$ or

$$QE = \gamma v, \tag{2}$$

where Q is the charge on the microtubule, E is the electric field strength, and γ is the drag coefficient. From the predicted charge on tubulin of 48 e^- per dimer (discussed above) a 10 μm microtubule will have a negative charge of 1.35×10^{-13} C. The drag coefficient for a cylinder aligned parallel to the direction of movement is (Howard, 2001, p. 107)

$$\gamma = \frac{2\pi\eta L}{\ln(L/2r) - 0.2}, \tag{3}$$

where η is the solution viscosity $(10^{-3}\,\text{N}\cdot\text{s/m}^2)$, L is the length of the microtubule (10 μm), and r is the microtubule radius (12 nm), giving $\gamma = 1.08 \times 10^{-8}\,\text{N}\cdot\text{s/m}$. The drag coefficient in the perpendicular direction is within a factor of two of this value. Hence, the predicted velocity of a 10 μm long microtubule in a 6×10^4 V/m electric field is

$$v = \frac{QE}{\gamma} \tag{4}$$

equal to 7.5×10^5 μm/s. Our measured velocity of 5 μm/s is five orders of magnitude smaller than this predicted velocity, so our measured electrophoretic forces are nowhere near the expected forces. One uncertainty here is the precise field strength at the plane of focus, but the most important factor is likely charge shielding by cations, which reduces the effective charge of the microtubule. Using a similar approach, Stracke et al. (2000, 2002) calculated the effective charge to be 0.19 e^- per tubulin dimer; we calculate the effective charge here to be in the range of $3 \times 10^{-4} e^-$ per tubulin dimer. In addition to these low forces, we also encountered problems in heating, electrolysis, and field-driven ion flows. These ion flows may be counteracting the electrophoretic forces; alternatively, we can't rule out that the observed microtubule movements are solely due to ion or convective flows. Because of these drawbacks we next investigated using dielectrophoresis to direct microtubules moving in channels.

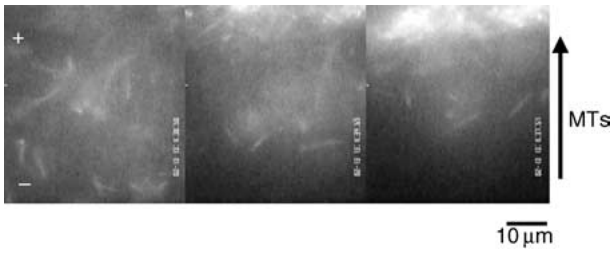

Fig. 6. *Movement of microtubules suspended in buffer towards the positive electrode in a 6 × 10⁴V/m DC electric field. The gap between the two electrodes is 50 μm, and the image sequence is 7 seconds total.*

Sorting microtubules by dielectrophoresis

Dielectrophoresis (DEP) provides a force related to the differential polarizability of the object of interest and the surrounding medium. Because cation shielding can be minimized by increasing the drive frequency to the point that ion motion is unable to follow the field signal, DEP reduces problems with heating and ion flows. Previously, we have used dielectrophoresis in combination with near field forces to move and position metallic and dielectric nanoparticles (Razavi et al., 2002), and there is a body of literature on manipulating cells and micron-scale beads by DEP forces (Pethig, 1997; Morgan et al., 1999; Hughes, 2002). There has been very little work to date on manipulating proteins by DEP (Washizu et al., 1994), though it has been recently reported that actin filaments can be organized and moved by dielectrophoresis (Asokan et al., 2003). We set out to determine whether microtubules can be manipulated by dielectrophoretic forces.

The dielectrophoretic force on a rod shaped particle in an electric field is given by (Pohl, 1978; Jones, 1995; Asokan et al., 2003):

$$F_{dep} = \left(\frac{\pi}{6} r^2 l\right) \varepsilon_m \alpha(\omega) \left(\nabla E_{rms}^2\right), \tag{5}$$

where r is the radius of the particle, l is the length, ε_m is the real permittivity of the surrounding medium, ∇ is the

gradient operator, E_{rms} is the local RMS electric field. $\alpha(\omega)$ is a factor indicating the effective polarizability of the particle and varies with the frequency of the applied field and the medium around the particle, as well as the properties of the particle itself (Pethig, 1997). Under a non-uniform AC field, microtubules are expected to move towards either the high electric field region (positive DEP) or the low electric field region (negative DEP) due to different polarizability of microtubules with respect to the surrounding media (buffers).

In addition to attractive forces, an electrical torque can be exerted on a dipole in an electric field, defined as

$$\tilde{T} = q\tilde{d} \times \tilde{E}, \tag{6}$$

where $\tilde{T}$ is torque vector, $\tilde{E}$ is electric field vector, $\tilde{d}$ is the distance vector between two opposite charges and q is the electrical charge at each end of the dipole. A dipole aligns itself along the field lines in response to a torque, which is termed electro-orientation (EO). In structurally asymmetric particles, EO can be used to align the particle axis with the electric field lines (Miller and Jones 1993).

Our eventual goal is to use DEP forces to redirect microtubule motion in microfabricated channels, but to characterize DEP forces on microtubules, we used a simple geometry—electrodes on surfaces and microtubules in solution. To model what behavior we might expect for microtubules in solution in an AC electric field, we simulated the electric field distribution for a pair of electrodes with a 10 µm gap using FEMLAB (Comsol, Inc.). Figure 7 shows the electric field distribution in the buffer just above the electrode surface where the highest field region is along the electrode edges. We then fabricated a pair of electrodes with a

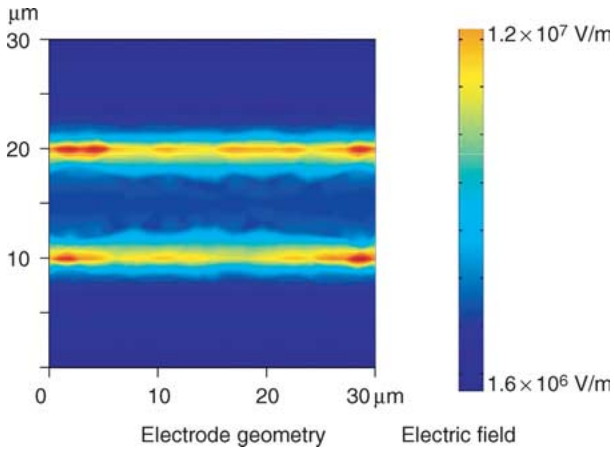

Fig. 7. *Simulation of the electric field distribution in BRB12 buffer just above the electrode surface using FEMLAB. The electrodes are in parallel and 10 µm apart. The high field region is along the edges of the two parallel electrodes.*

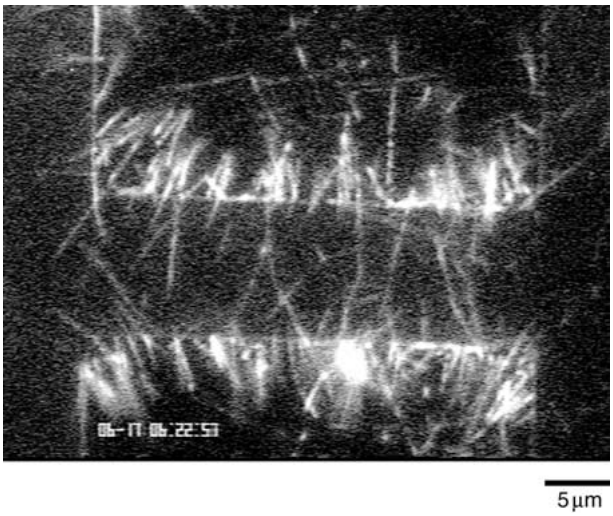

Fig. 8. *Alignment of microtubules in the high field region by dielectrophoresis. The applied signal was 50 $V_{P\text{-}P}$, frequencey was 20 kHz, and predicted field strength was 5.0 × 10^6 V/m.*

10 µm gap and applied a 20 kHz AC field with amplitude 50 $V_{P\text{-}P}$. When the AC field was turned on, microtubules were observed moving toward the edges of the two electrodes and remaining there (Figure 8), some filaments were even aligned across the gap between the two electrodes, presumably due to electro-orientation. We varied the frequency from 1 kHz to 1 MHz and found no negative DEP. Hence, DEP successfully moved and aligned microtubules in solution, indicating that this approach may be feasible for redirecting microtubule motions in microfabricated channels.

Transporting nanowires

In cells, kinesins move along immobilized microtubules, opposite to the microtubule transport geometry discussed above. We sought to exploit the geometry used by cells to transport and organize nano- and micro scale material for directed assembly. From biophysical measurements on motor proteins, it has been established that motors can transport micronscale glass or polystyrene beads along microtubules at speeds of ~ 0.5 µm/s (Howard et al., 1989) and generate unitary motor forces on the order of 7 pN per molecule (Schnitzer et al. 2000). Furthermore, Limberis and Stewart (2000) have observed rotational movement of 10 µm silicon chips powered by kinesin on microtubule functionalized glass surfaces. Here we extend this to show that motors can transport high aspect ratio gold nanowires over long distances.

Gold nanowires were grown by electroplating gold in porous membranes (Martin et al., 1999) and then dissolving the membrane with ethanol to release the nanowires. This approach has been established by Mallouk, Keating and other groups to produce high

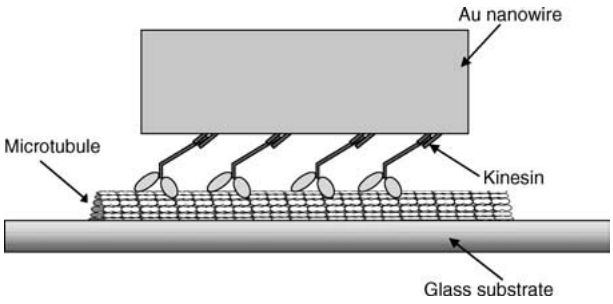

Fig. 9. *Schematic of Au nanowire movement powered by kinesin on immobilized microtubules.*

aspect ratio nanowires with diameters down to 10 s. of nm and lengths up to microns from not only gold but also platinum, zinc and other metals (Mbindyo et al., 2001). This tight control over synthesis offers the hope that they could be interconnected as a step towards ''bottom-up'' electronics assembly (Kovtyukhova and Mallouk, 2002), possibly providing an alternative or adjunct to traditional microelectronics fabrication techniques. However, the key hurdle is manipulating and organizing these wires into useful spatial arrangements.

Figure 9 shows the schematic of kinesin coated Au nanowires moving on immobilized microtubules. To functionalize the nanowires with motors, the wires were pelleted and resuspended in BRB80 buffer, then mixed with 1 mg/ml casein for 10 minutes to passivate the surface, followed by a 30-minute incubation on ice with 0.8 nM kinesin in 10 μM ATP. To immobilize microtubules, glass coverslips were treated with APTES (3-Aminopropyltriethoxysilane, PIERCE, Rockford, IL) (Svoboda et al., 1993) and assembled into a flow cell. The amino groups of APTES create a positively charged surface that binds to the negatively charged microtubules. Microtubules were immobilized by flowing them into the flow cell, incubating for 3 minutes and washing out any excess. Finally, the kinesin-coated nanowire suspension was injected into the flow cell and the movement was observed by DIC microscopy.

Kinesin-driven nanowire motility is shown in Figure 10. The clump consists of tens of nanowires 200 nm in diameter and 6 μm long. The assemblage traveled across the screen over 50 μm in 80 seconds for a mean speed of 0.6 μm/s, similar to the speed of free microtubules moving over immobilized kinesin. Hence, kinesins can be functionally adsorbed to these gold surfaces, the motors can transport the wires along immobilized filaments, and the high speed indicates that the wires provide a negligible load for the motors.

Despite this long distance movement, the direction of nanowire movement is random because the microtubules are immobilized randomly on the glass surfaces. It has been previously demonstrated that an array of oriented

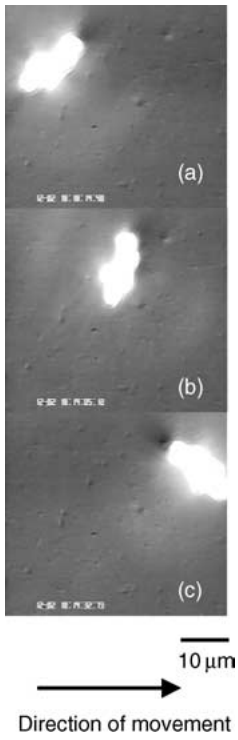

Fig. 10. *The movement of a Au nanowire clump a microtubule-functionalized surface observed by differential interference contrast microscopy.*

microtubules can be created by growing microtubules from immobilized seeds and orienting them by flow (Brown and Hancock, 2002). By transporting the nanowires along such a polarized array, unidirectional motion could be achieved, and microtubule tracks oriented perpendicular to this original array could be used to build junctions between nanowires. Work is ongoing to immobilize microtubules on surfaces and in channels to better control this nanowire movement and assembly.

Conclusions and Future Work

We have created microfabricated channels functionalized with kinesin motors to direct, reorient, and sort moving microtubules. Arrowhead patterns successfully redirected microtubules moving in channels, but further design is needed to optimize arrowhead geometries. In solution, microtubules could be manipulated by both DC and AC electric fields, but the calculated forces of DC fields were considerably less than predicted and at higher field strengths heating and electrolysis became a problem. The next step is to fabricate the electrodes into channels to test whether microtubules can be properly sorted at bifurcations. In addition LEDs and

photodiodes will be encapsulated into the channel walls to detect fluorophores moving in the channels. Finally, work is ongoing to functionalize microtubules to bind specific DNA, protein, or cellular cargo for sensing, analysis or purification. Because biomolecular motors can specifically transport analytes in the absence of fluid flow, and the channels can be scaled down to the 25 nm dimensions of the microtubules, this work paves the way for a new class of hybrid biological/engineered microdevices powered by biomolecular motors.

Acknowledgments

This project was funded by DARPA, Whitaker Foundation and the Penn State Center for Nanoscale Science (NSF MRSEC). We also thank S.K. St. Angelo (Mallouk Lab, Department of Chemistry), for providing gold nanowires and Yangrong Zhang for purifying kinesin.

References

1. R.D. Allen, N.S. Allen, and J.L. Travis, Cell Motil **1**, 291 (1981).
2. S.B. Asokan, L. Jawerth, R.L. Carroll, R.E. Cheney, S. Washburn, and R. Superfine, Nano Letters **3**, 431 (2003).
3. T.B. Brown and W.O. Hancock, Nano Letters **2**, 1131 (2002).
4. J. Clemmens, H. Hess, J. Howard, and V. Vogel, Langmuir **19**, 1738 (2003).
5. D.L. Coy, M. Wagenbach, and J. Howard, J. Biol. Chem. **274**, 3667 (1999).
6. J.R. Dennis, J. Howard, and V. Vogel, Nanotechnology **10**, 232 (1999).
7. R.W. Fitzgerald, *Mechanics of Materials* (Addison-Wesley, Reading, MA, 1982), p. 554.
8. F. Gittes, B. Mickey, J. Nettleton, and J. Howard, J. Cell. Biol. **120**, 923 (1993).
9. D.D. Hackney, Proc. Natl. Acad. Sci. (USA) **85**, 6314 (1988).
10. W.O. Hancock and J. Howard, J. Cell. Biol. **140**, 1395 (1998).
11. H. Hess, J. Clemmens, D. Qin, J. Howard, and V. Vogel, Nano Letters **1**, 235 (2001).
12. Y. Hiratsuka, T. Tada, K. Oiwa, T. Kanayama, and T.Q. Uyeda, Biophys. J. **81**, 1555 (2001).
13. J. Howard, *Mechanics of Motor Proteins and the Cytoskeleton* (Sinauer Associates, Inc., Sunderland, MA, 2001).
14. J. Howard, A.J. Hudspeth, and R.D. Vale, Nature **342**, 154 (1989).
15. J. Howard, A.J. Hunt, and S. Baek, Methods Cell. Biol. **39**, 137 (1993).
16. M.P. Hughes, Electrophoresis **23**, 2569 (2002).
17. A. Hyman, D. Drechsel, D. Kellogg, S. Salser, K. Sawin, P. Steffen, L. Wordeman, and T. Mitchison, Methods Enzymol. **196**, 478 (1991).
18. T.B. Jones, *Electromechanics of Particles* (Cambridge University Press, 1995).
19. N.I. Kovtyukhova and T.E. Mallouk, Chemistry **8**, 4354 (2002).
20. L. Limberis and R.J. Stewart, Nanotechnology **11**, 47 (2000).
21. J. Lowe, H. Li, K.H. Downing, and E. Nogales, J. Mol. Biol. **313**, 1045 (2001).
22. S.A. Marras, F.R. Kramer, and S. Tyagi, Genet. Anal. **14**, 151 (1999).
23. B.R. Martin, D.J. Dermody, B.D. Reiss, M. Fang, L.A. Lyon, M.J. Natan, and T.E. Mallouk, Adv. Mater. **11**, 1021 (1999).
24. J.K.N. Mbindyo, B.D. Reiss, B.R. Martin, C.D. Keating, M.J. Natan, and T.E. Mallouk, Adv. Mater. **13**, 249 (2001).
25. E. Meyhöfer and J. Howard, Proc. Natl. Acad. Sci. (USA) **92**, 574 (1995).
26. R.D. Miller and T.B. Jones, Biophys. J. **64**, 1588 (1993).
27. S.G. Moorjani, L. Jia, T.N. Jackson, and W.O. Hancock, Nano Letters **3**, 633 (2003).
28. H. Morgan, M.P. Hughes, and N.G. Green, Biophys. J. **77**, 516 (1999).
29. E. Nogales, M. Whittaker, R.A. Milligan, and K.H. Downing, Cell **96**, 79 (1999).
30. R.a.M. Pethig, G.H. Markx, Trends in Biotechnology **15**, 426 (1997).
31. H.A. Pohl, *Dielectrophoresis: The Behavior of Neutral Matter in Non-Uniform Electric Fields* (Cambridge University Press, 1978).
32. B. Razavi, B.R. Martin, S.K. St. Angelo, T.E. Mallouk, and T.N. Jackson, 44th Electronic Materials Conference Digest (2002).
33. M. Schena, D. Shalon, R.W. Davis, and P.O. Brown, Science **270**, 467 (1995).
34. M.J. Schnitzer, K. Visscher, and S.M. Block, Nat. Cell. Biol. **2**, 718 (2000).
35. R. Stracke, K.J. Bohm, J. Burgold, H.-J. Schacht, and E. Unger, Nanotechnology **11**, 52 (2000).
36. R. Stracke, K.J. Bohm, L. Wollweber, J.A. Tuszynski, and E. Unger, Biochem. Biophys. Res. Commun. **293**, 602 (2002).
37. K. Svoboda, C.F. Schmidt, B.J. Schnapp, and S.M. Block, Nature **365**, 721 (1993).
38. R.D. Vale, B.J. Schnapp, T.S. Reese, and M.P. Sheetz, Cell **40**, 559 (1985).
39. M. Washizu, S. Suzuki, O. Kurosawa, T. Nishizaka, and T. Shinohara, IEEE Transactions on Industry Applications **30**, 835 (1994).
40. R.C. Williams, Jr. and J.C. Lee, Methods Enzymol. **85 Pt B**, 376 (1982).